ACS Macro Letters

Letter

pubs.acs.org/macroletters

Strain Hardening During Uniaxial Compression of Polymer Glasses

Panpan Lin, Shiwang Cheng, and Shi-Qing Wang*

Maurice Morton Institute of Polymer Science and Engineering, University of Akron, Akron, Ohio 44325-3909, United States

ABSTRACT: The origin of high mechanical stresses in large deformation of polymer glasses has been elusive because both plasticity and elasticity take place. In this work on the nature of the mechanical responses, we carry out uniaxial compression experiments to make simultaneous mechanical and thermal measurements of polycarbonate. Our results confirm that two factors contribute to the growing mechanical stress in the post-yield regime, which is known as "strain hardening". Besides plastic deformation that is intersegmental in origin, chain tension as an intrasegmental component contributes considerably to the measured stress in post-yield. Such a conclusion modifies the previous consensus regarding the nature of strain hardening in mechanical deformation of polymer glasses.

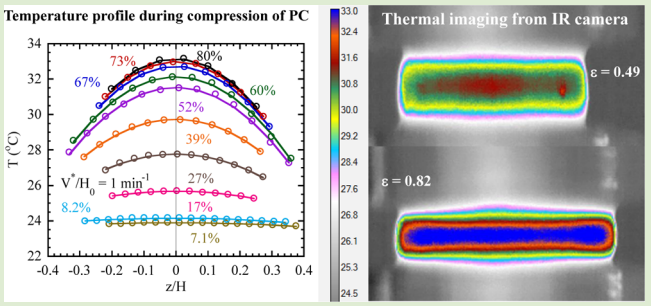

Long polymer chains form a temporary (entanglement) network above the glass transition temperature T_g that reconstructs over time by molecular diffusion. Upon vitrification, that is, thermal quenching below T_g, all chain segments become spatially "frozen" to form a rigid primary structure percolating throughout the system in the absence of external deformation and giving rise to high Young's modulus. In addition, a chain network is also present in the glassy state. Understanding the role of such a chain network and the interplay between the primary structure and chain network is key to controlling the toughness of polymer glasses.[1] Polymer glasses of high molecular weight can undergo uniform compression even after yielding to attain high compression ratios. More remarkably, the mechanical stress can monotonically increase with deformation in the post-yield regime, which is known as strain hardening.

Concerning the molecular origin of such a strain hardening phenomenon, various mechanisms have been proposed in the past four decades. Besides constitutive modeling,[2] earlier studies interpreted the strain hardening as due to entropic rubber elasticity.[3−6] On the other hand, experiments[7,8] indicate that the idea of entropic rubber elasticity as the stress origin in polymer glasses is incorrect. As emphasized by Kramer,[9] the explanation based on rubber elasticity contradicts the fact that the hardening modulus G_R is much higher than the melt plateau modulus G_N^0. Recent computer simulations[10−17] have begun to clarify the controversy by showing that large deformation behavior in uniaxial compression is dominantly plastic although there is a sign of energetic contributions at the highest strains. It is suggested that the dissipative plastic deformation produces higher stress when the chain energetic stretching causes the rate of plastic rearrangements to increase. DSC measurements of enthalpy release revealed appreciable internal energy storage associated with microstructural rearrangement.[18] Infrared detection of heat release also indicated measurable energy storage in the post-yield regime.[19] Moreover, statistical mechanical theories have been developed to probe the origin of mechanical stress during large deformation of polymer glasses.[20−25]

The objective of the present work is to investigate whether intrasegmental effects are important during uniaxial compression of polymer glasses. We combine conventional mechanical measurements with in situ video recording of the specimen's spatial temperature profile using an IR camera. Figure 1 shows four video frames of the temperature rise during compression with an initial Hencky rate of $V^*/H_0 = 1\ \mathrm{min}^{-1}$, where V^* is the crosshead speed and remains constant during compression, and H_0 is the initial sample height. The middle colorful part represents the cylindrical PC specimen. Various colors indicate different temperatures, as shown in the color scheme. The thermal imaging of Figure 1 allows us to map out a one-dimensional temperature variation along the sample height direction z. As an example, Figure 2 shows a set of nearly symmetric temperature profiles during 10 different stages of the uniaxial compression with an initial strain rate of $V^*/H_0 = 1\ \mathrm{min}^{-1}$.

The specimen's temperature increases because of the heat generation, associated with the change of energy landscape by the externally imposed compression. Specifically, the temperature field obeys the following heat equation

$$\rho c_p \frac{\partial T(z,t)}{\partial t} = \kappa \frac{\partial^2 T(z,t)}{\partial z^2} + \dot{q} \qquad (1)$$

where ρ is the mass density, c_p is the specific heat capacity, T is the sample temperature, κ is the thermal conductivity, and $\dot{q}$ is the source, that is, the rate of heat release per unit volume.

Received: July 7, 2014
Accepted: July 23, 2014
Published: July 24, 2014

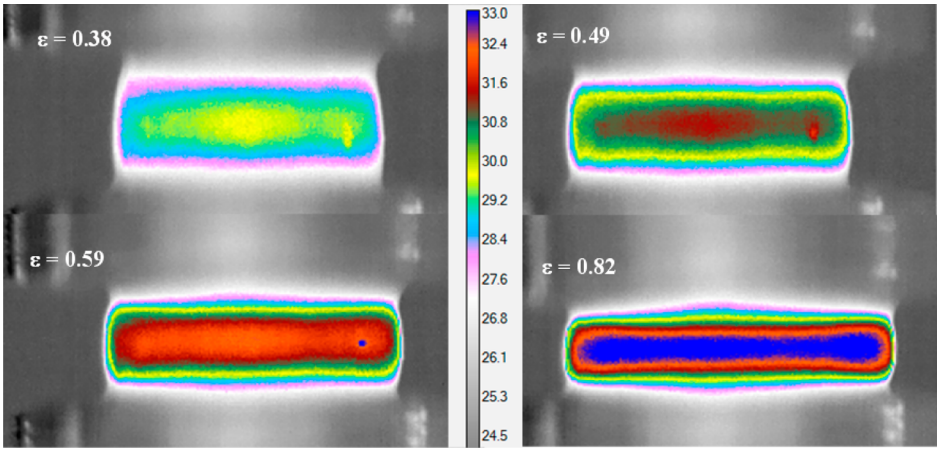

Figure 1. Four images of the temperature profile during compression of a PC specimen (initial cylindrical dimensions: 5.7 mm in diameter and height H_0 = 5.9) at an initial rate of V^*/H_0 = 1 min^{-1}, captured with an IR camera.

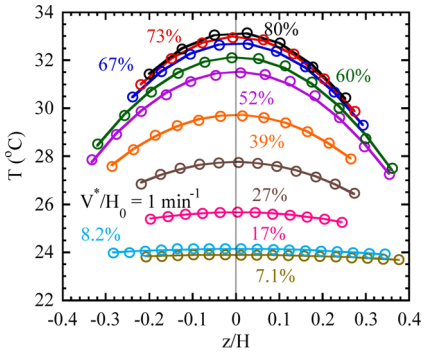

Figure 2. Temperature profiles across the specimen at different stages during the compression at V^*/H_0 = 1 min^{-1}.

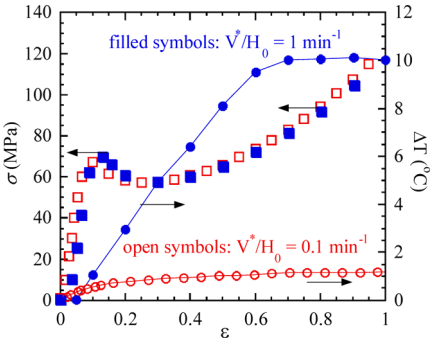

Figure 3. Stress–strain curves (squares) and the corresponding temperature-strain curves (circles) during uniaxial compression, performed with Instron 5567 with initial rates V^*/H_0 = 1 min^{-1} (filled symbols) and V^*/H_0 = 0.1 min^{-1} (open symbols) respectively, where $\Delta T = (T_{max} - T_a)$, with T_a being the ambient temperature equal to 23 °C and $T_{max} = T(z = 0, t)$ the temperature reading at the middle of the specimen. The initial dimensions of these cylindrical specimens are 5.7 mm in diameter with height H_0 = 5.9 mm and 5.3 mm in diameter with H_0 = 5.4 mm, respectively.

The heat release rate $\dot{q}$ appears in the second law of thermodynamics,[26] in the case of uniaxial compression, as follows,

$$\sigma\dot{\varepsilon} = \dot{q} + \dot{u} + \Delta \tag{2}$$

which states that the external work density per unit time, $\sigma\dot{\varepsilon}$, results in heat generation $\dot{q}$, internal energy increase $\dot{u}$, and internal dissipation Δ. Here σ is the tensile stress and $\dot{\varepsilon}$ is the Hencky strain rate. The simultaneous mechanical measurements produce the tensile stress vs strain curves as shown in Figure 3 at initial strain rates of 1 and 0.1 min^{-1}, respectively, where also plotted is the specimen's maximum temperature change at z = 0 as a function of time.

The nature of the mechanical responses can be delineated by determining how the external work is partially stored as internal energy and partially dissipated. To do so, we rewrite eq 2 to express the total stress as a sum of three terms

$$\sigma = (\dot{q} + \Delta)(H/V^*) + \dot{u}/\dot{\varepsilon} \equiv \sigma_q + \sigma_{ID} + \partial u/\partial\varepsilon \tag{3}$$

where σ_q is associated with the measurable heat generation, σ_{ID} denotes the internal dissipation. The last term, $\partial u/\partial\varepsilon$, represents an elastic component of the mechanical stress, which should be intrasegmental in origin. One purpose of the present work is to determine the magnitude of $\partial u/\partial\varepsilon$ relative to σ by simultaneous measurements of σ and σ_q.

We evaluate $\sigma_q = \dot{q}(H/V^*)$ in eq 2 according to eq 1 and Figure 2. For PC, the density ρ equals 1200 kg/m^3, κ = 0.20 $W/(m{\cdot}K)$, the specific heat c_p can be taken as a constant equal to c_p = 1200 J/(kg·K) because the temperature increase from 23 °C up to 33 °C during compression does not appreciably affect c_p. For uniform compression, the stress is homogeneous, and the heat generation is the same everywhere in the specimen. In other words, $\sigma_q \sim \dot{q}$ is constant independent of z. Thus, we can estimate $\dot{q}$ based on the information at z = 0. Figure 4 shows σ_q in open symbols for two speeds of V^* = 0.1 and 1 min^{-1}, along with the total stress σ given by the two smooth curves. The data for V^* = 1 min^{-1} look ordinary in the sense that $\sigma_q < \sigma$, as expected. On the other hand, the circles in Figure 4 show surprising behavior relative to the red (online) curve. In other words, we observed the heat release rate in the post-yield regime at a level higher than the rate of external work. For $\sigma_q > \sigma$ to occur, we must have $\partial u/\partial\varepsilon < 0$ in eq 3 since σ_{ID} cannot be negative. Thus, there must have been an internal energy build-up prior to the point of $\sigma_q > \sigma$ because the overall internal energy of the PC glass cannot decrease from its value of the undeformed state. Such internal energy storage due to external deformation is consistent with the idea that distortion of chain configuration may have occurred at the bond level.[27,28] Therefore, the difference between the circles and curve means that beyond the yield point relaxation of some

dx.doi.org/10.1021/mz5004129 | ACS Macro Lett. 2014, 3, 784–787

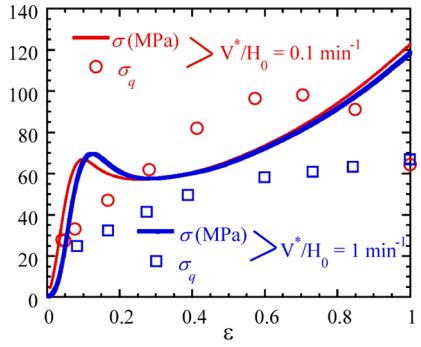

Figure 4. Dissipative component σ_q of the total stress σ associated with the heat release during compression in Instron 5567 at V^*/H_0 = 0.1 and 1 min^{-1}, respectively. Also presented is the total stress σ given by the two continuous curves.

intrasegmental deformation has taken place in the form of released heat as the glassy state returns to a lower energy state.

We can verify that there is overall energy conservation. We evaluate the total specific mechanical work (i.e., work done to the sample per unit volume) and specific heat release by integrating the data of σ and σ_q in Figure 4 to get

$$w = \int_0^{\varepsilon} \sigma(\varepsilon)\mathrm{d}\varepsilon \tag{4a}$$

and

$$q = \int_0^{t} \dot{q}(s)\mathrm{d}s \equiv \int_0^{\varepsilon} \sigma_q(\varepsilon)\mathrm{d}\varepsilon \tag{4b}$$

In Figure 5 we plot w and q, respectively, as a function of the strain ε for both rates. Here the continuous curve represents

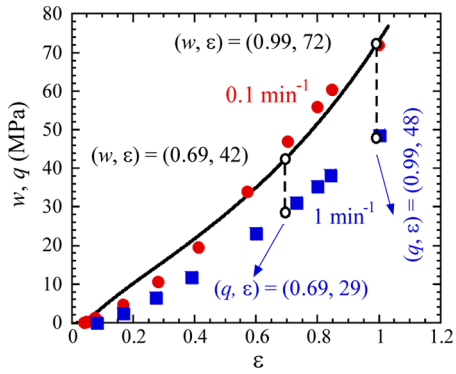

Figure 5. External work in the continuous curve as well as the measured heat release in solid symbols per unit volume as a function of the compressive strain for both V^*/H_0 = 0.1 (circles) and 1 (squares) min^{-1}.

the work density w, which is essentially the same at these two rates, and the solid symbols are the total heat generations per unit volume at each stage of the compression at V^*/H_0 = 0.1 and 1.0 min^{-1}, respectively. Since the circles essentially fall on top of the curve, it confirms that there is not more heat generated than the input mechanical energy. The data above the curve are indicative of the level of experimental error. More interestingly and importantly, the squares stay appreciably below the curve. The remaining of this Letter focuses on the implication of this difference between the smooth curve and squares for 1 min^{-1}.

Data in both Figures 4 and 5 indicate that $(\sigma - \sigma_q) > 0$ at all times during the compression with rate V^*/H_0 = 1 min^{-1}. If σ_{ID} is negligible, such data imply that the internal energy keeps building up because $\partial u/\partial\varepsilon \sim (\sigma - \sigma_q) > 0$. In other words, there is a significant intrasegmental contribution to the total stress. In our recent molecular picture,[1] it means that deformation of a chain network also takes place, giving rise to chain tension buildup in the load-bearing strands. To determine whether σ_{ID} is indeed insignificant or not, we carry out an independent evaluation of the internal energy based on differential scanning calorimetric (DSC) measurements of the compressed PC at an initial strain rate of 1 min^{-1} to two Hencky strains of ε = 0.69 and 0.99, respectively. The internal energy buildup during the compression can be detected when subjecting the sample to the DSC measurements.[18,29,30] Specifically, upon heating the internal energy will be released, corresponding to the restoration of any distortion of bond angle and length, so that the heat flow required to warm up the specimen will be lower. Figure 6a,b indicates that there is indeed internal energy release as shown by the difference in the area under the heat flow curves between the first and second cycles. Equating the difference to the internal energy per unit volume u, we find u = 13.2 MPa at ε = 0.69 and 24.9 MPa at ε = 0.99, respectively. These values match the difference observed in Figure 5 between w and q. In other words, the observation of $u \sim (w - q)$ implies σ_{ID} in eq 3 is negligible because of the definitions given in eqs 4a and 4b. Thus, we conclude that our temperature measurements by the IR camera essentially account for the total energy dissipation and can be used to evaluate the energetic component of the mechanical stress.

In summary, the simultaneous mechanical and thermal measurements for uniaxial compression of the ductile PC in conjunction with the post-compression DSC measurements not only provided two independent evaluations of the internal energy storage but also allowed us to conclude that the internal dissipation is a negligible fraction. Moreover, for our low rate compression, it is necessary to obtain the temperature profile because the thermal conduction term, that is, the first term on the right-hand side of eq 1, is actually dominant over that associated with the temperature rise of the compressed specimen. According to our results, we conclude that there are two factors contributing to the observed growing stress in the post-yield regime. (a) More segments participate in plastic flow, that is, sliding past one another and slipping around junctions of the chain network. (b) More bond distortions (e.g., bond stretching and bond angle distortion) take place as the intrasegmental backbone tension further increases. Such chain tension has been shown to produce the elastic yielding.[28,31] In closing, it is important to note that excessive heat release (circles above the continuous curve in Figure 4) is consistent with the idea that internal energy is stored during deformation.[10,18,19,29,30] When it is released in the form of heat, the glassy state has arrived at a lower energy state, presumably due to recovery from the bond distortions and configurational transitions such as the *gauche*−*trans* transition. More study is needed to examine the rate effect seen in Figure 4. Our current explanation is that at the lower rate the bond tension has time to overcome the confining barrier, resulting in the excessive heat release, with the circles rising above the continuous stress curve.

dx.doi.org/10.1021/mz5004129 | ACS Macro Lett. 2014, 3, 784−787

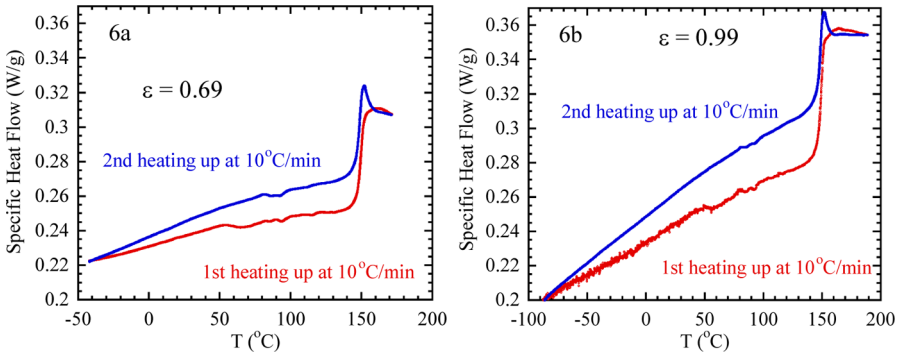

Figure 6. DSC measurements of two samples compressed to two different Hencky strains of (a) $\varepsilon = 0.69$ and (b) $\varepsilon = 0.99$ at $V^*/H_0 = 1\ \text{min}^{-1}$.

EXPERIMENTAL METHODS

This study is based on a bisphenol A polycarbonate (PC) from Sabic (Lexan TM 141 111), which has a weight-averaged molecular weight of 63 kg/mol and polydispersity of 1.58. The molecular weight is determined by a chloroform-based TOSOH EcoSEC HLC-8320 GPC, with two TSK-GEL^R Super H 3000 columns and one TSK-GEL^R Super H 4000 column in series.

The specimens were prepared by extrusion at around 215 °C through a capillary die of a large diameter that produces an extrudate with a diameter of about 5.5 mm. Such an extrudate is cut to a height of about 5.5 mm before being placed between two compression plates with lubricant oil between the cylinder-shaped specimen and the compress plates. Uniaxial compression was performed on Instron 5567, along with an infrared camera FLIR SC325 operated at 60 Hz to in situ measure the temperature profile. DSC measurements were carried out with a TA Q2000 DSC at a heating rate of 10 °C/min.

AUTHOR INFORMATION

Corresponding Author

*E-mail: swang@uakron.edu.

Notes

The authors declare no competing financial interest.

ACKNOWLEDGMENTS

The work is, in part, supported by ACS-PRF (54047-ND7) as well as NSF-DMR (EAGER-1444859).

REFERENCES

(1) Wang, S. Q.; Cheng, S.; Lin, P.; Li, X. *J. Chem. Phys.* **2014**, in press.
(2) Haward, R. N.; Thackray, G. *Proc. R. Soc. London, Ser. A* **1968**, *302*, 453−472.
(3) Argon, A. S. *Philos. Mag.* **1973**, *28*, 839−865.
(4) Argon, A. S. *J. Macromol. Sci. Phys.* **1973**, *8*, 573−596.
(5) Cross, A.; Haward, R. N. *Polymer* **1978**, *19*, 677−82.
(6) Boyce, M. C.; Parks, D. M.; Argon, A. S. *Mech. Mater.* **1988**, *7*, 15−33.
(7) van Melick, H. G. H.; Govaert, L. E.; Meijer, H. E. H. *Polymer* **2003**, *44*, 2493−2502.
(8) Govaert, L. E.; Tervoort, T. A. *J. Polym. Sci., Polym. Phys.* **2004**, *42*, 2041−2049.
(9) Kramer, E. J. *J. Polym. Sci., Polym. Phys.* **2005**, *43*, 3369−3371.
(10) Hoy, R. S.; Robbins, M. O. *Phys. Rev. Lett.* **2007**, *99*, 117801.
(11) Hoy, R. S.; Robbins, M. O. *Phys. Rev. E* **2008**, *77*, 031801.
(12) Barrat, J.-L.; Baschnagel, J.; Lyulin, A. *Soft Matter* **2010**, *6*, 3430−3446.
(13) Rottler, J. *J. Phys. Condens. Mater.* **2009**, *21*, 463101.
(14) Vorselaars, B.; Lyulin, A. V.; Michels, M. A. J. *J. Chem. Phys.* **2009**, *130*, 074905.
(15) Ge, T.; Robbins, M. O. *J. Polym. Sci., Polym. Phys.* **2010**, *48*, 1473−1482.
(16) Hoy, R. S.; O'Hern, C. S. *Phys. Rev. E* **2010**, *82*, 041803.
(17) Hoy, R. S. *J. Polym. Sci., Polym. Phys.* **2011**, *49*, 979−984.
(18) Hasan, O. A.; Boyce, M. C. *Polymer* **1993**, *34*, 5085−5092.
(19) Garg, M.; Mulliken, A. D.; Boyce, M. C. *J. Appl. Mech.* **2008**, *75*, 011009.
(20) Chen, K.; Schweizer, K. S. *Phys. Rev. Lett.* **2009**, *102*, 038301.
(21) Chen, K.; Schweizer, K. S. *Europhys. Lett.* **2007**, *79*, 26006.
(22) Chen, K.; Schweizer, K. S. *Macromolecules* **2008**, *41*, 5908−5918.
(23) Chen, K.; Saltzman, E. J.; Schweizer, K. S. *J. Phys. Condens. Mater.* **2009**, *21*, 503101.
(24) Chen, K.; Saltzman, E. J.; Schweizer, K. S. *Annu. Rev. Condens. Matter Phys.* **2010**, *1*, 277−300.
(25) Chen, K.; Schweizer, K. S. *Macromolecules* **2011**, *44*, 3988−4000.
(26) Haupt, P.; Kurth, J. A. *Continuum Mechanics and Theory of Materials*; Springer: New York, 2010.
(27) Crist, B. In *The Physics of Glassy Polymers*, 2nd ed.; Haward, R. N., Young, R. J., Eds.; Chapman & Hall: London, 1997.
(28) Cheng, S.; Wang, S.-Q. *Phys. Rev. Lett.* **2013**, *110*, 065506.
(29) Chang, B. T. A.; Li, J. C. M. *Polym. Eng. Sci.* **1988**, *28*, 1198−202.
(30) Adams, G. W.; Farris, R. J. *J. Polym. Sci., Polym. Phys.* **1988**, *26*, 433−445.
(31) Cheng, S.; Wang, S.-Q. *Macromolecules* **2014**, *47*, 3661−3671.